

Extreme nonlinear electrodynamics in metamaterials with very small linear dielectric permittivityA. Ciattoni,¹ C. Rizza,² and E. Palange²¹*Consiglio Nazionale delle Ricerche, CNR-SPIN, I-67100 L'Aquila, Italy and Dipartimento di Fisica, Università dell'Aquila, I-67100 L'Aquila, Italy*²*Dipartimento di Ingegneria Elettrica e dell'Informazione, Università dell'Aquila, I-67100 Monteluco di Roio (L'Aquila), Italy*
(Received 18 February 2010; published 28 April 2010)

We consider a subwavelength periodic layered medium whose slabs are filled by arbitrary linear metamaterials and standard nonlinear Kerr media and show that the homogenized medium behaves as a Kerr medium whose parameters can assume values not available in standard materials. Exploiting such a parameter availability, we focus on the situation where the linear relative dielectric permittivity is very small, thus allowing the observation of the extreme nonlinear regime where the nonlinear polarization is comparable with or even greater than the linear part of the overall dielectric response. The behavior of the electromagnetic field in the extreme nonlinear regime is very peculiar and characterized by interesting features such as the transverse power flow reversing. In order to probe this regime, we consider a class of fields (transverse magnetic nonlinear guided waves) admitting full analytical description and show that these waves are allowed to propagate even in media with $\epsilon < 0$ and $\mu > 0$ since the nonlinear polarization produces a positive overall effective permittivity. The considered nonlinear waves exhibit, in addition to the mentioned features, a number of interesting properties like hyperfocusing induced by the phase difference between the field components.

DOI: [10.1103/PhysRevA.81.043839](https://doi.org/10.1103/PhysRevA.81.043839)

PACS number(s): 42.65.Tg, 78.67.Pt

I. INTRODUCTION

Electromagnetic propagation through metamaterials has stimulated, since the early 2000s, intense research activity with two main purposes: the identification of artificial structures exhibiting anomalous values of the permittivity ϵ and the permeability μ [1,2] and the investigation of the electromagnetic phenomenology resulting from the unusual electromagnetic properties. Leading examples of the class of phenomena supported by metamaterials are superlensing [3,4], optical cloaking [5,6], and photonic circuits [7]. Recently, a good deal of attention has been devoted to the investigation of metamaterials characterized by a very small dielectric permittivity (ϵ -near-zero materials) since they host an electromagnetic regime where the magnetic field displays static features [8] and the tunneling of electromagnetic energy through subwavelength channels has been proposed [9] and experimentally observed [10,11]. Metamaterials exhibiting remarkable nonlinear properties have been investigated as well [12] and various soliton manifestations [13–16] have been considered. The investigation of metamaterial nonlinear properties is particularly important in that it can lead to overcoming one of the fundamental limits of nonlinear optics: the fact that most of the optical materials have a relatively weak nonlinear response. The main idea is that the local electromagnetic fields of the inclusions in the metamaterial can be much larger than the average value of the field thus producing an enhancement of the nonlinear response [17–19]. The problem of achieving a substantial enhancement of the nonlinear response has also been considered within the more general subject of composite structures homogenization [20–24], and the strategy is always that of conceiving a microscopic inhomogeneous structure concentrating the field within the nonlinear constituents.

The full exploitation of the nonlinear response is possible only if the nonlinear polarization is not a small perturbation to the linear part of the electric displacement field, and generally this is achieved through nonlinearity enhancement

or by means of resonant processes or photorefractive processes where the large nonlinearities come at the cost of a large time response. However, as shown in this article, the interplay between the linear part of the electric displacement field and the nonlinear polarization can be made efficient even by following the opposite route, i.e., by reducing the linear polarization. We therefore devise a nonlinear medium with a very small linear dielectric constant since it is a natural setting for the observation of the electromagnetic regime where the nonlinear response does not play the role of a mere perturbation.

In this article we consider a periodic layered composite whose slabs are filled either with linear media with arbitrary permittivity and permeability or by standard isotropic focusing or defocusing Kerr media. Exploiting a suitable extension of the well-known technique generally used for describing the homogenization of linear layered composites, we show that the homogenized medium is characterized by effective constitutive relations formally coinciding with those of a standard Kerr medium. We note that the parameters characterizing such an effective response can be simply tailored through a suitable choice of the composite underlying constituents and that, due the large freedom in choosing both constituent media and their volume filling fraction, the design of linear and nonlinear properties can be independently performed. Therefore our composite medium allows a full and efficient engineering of the Kerr nonlinear response. More interestingly, we prove that the effective response parameters span very wide ranges encompassing values not available in standard media. The standard isotropic Kerr response (in the the frequency domain) generally depends on two parameters usually denoted with A and B [25] in term of which we define $\chi = A$ and $\gamma = B/2A$ and the available values of γ belong to the range $0 < \gamma < 3$ (depending on the actual mechanism supporting the Kerr response). In this article we prove that the parameter γ appearing in the effective Kerr nonlinear response can, in principle, assume any value (encompassing negative and very

large values) and we discuss the impact of the exotic values of γ on the electromagnetic phenomenology.

Confining our attention to transverse magnetic (TM) fields, we show that it is possible to design a nonlinear Kerr medium whose linear dielectric permittivity is much smaller than 1 and therefore able to host the electromagnetic regime where nonlinearity cannot be regarded as a perturbation (extreme nonlinear regime). As a first general electromagnetic effect characteristic of the extreme nonlinear regime, we discuss the transverse power flow reversing, i.e., the fact that, for an electromagnetic beam, the Poynting vector on the beam propagation axis can be antiparallel to Poynting vector on the beam lateral sides [26]. Within the extreme nonlinear regime, the full exploitation of the nonlinear response can be achieved and, in order to discuss the consequent electromagnetic phenomenology, we consider a class of nonlinear guided waves admitting full analytical treatment. A number of the obtained nonlinear guided waves exhibit, as expected, transverse power flow reversing. We prove that, in the situation where $\epsilon < 0$, $\mu > 0$ and $\chi > 0$ (or in the equivalent case $\epsilon > 0$, $\mu < 0$ and $\chi < 0$) these waves are allowed to propagate through the medium if $-1 < \gamma < 0$, in striking contrast to the fact that, in a linear medium with the same permittivity and permeability, any wave would be evanescent. This is possible since nonlinearity overcomes the linear contribution to the electric displacement field producing an effective nonlinear dielectric permittivity able to support propagating waves. In addition we identify a mechanism which, combining the extreme nonlinear regime with the properties of the effective medium response with $\gamma \simeq -1$, produces a hyperfocusing of the considered nonlinear guided waves. In the situation $\epsilon > 0$, $\mu > 0$ and $\chi < 0$ (or in the equivalent case $\epsilon < 0$, $\mu < 0$ and $\chi > 0$) the nonlinear guided waves exist in the wider range $-\infty < \gamma < -1$ and $0 < \gamma < +\infty$ thus allowing to probe the Kerr nonlinear response for large values of $|\gamma|$. Since the phase difference between the components of the considered waves is $\pi/2$, we predict that, for $\gamma \rightarrow +\infty$, an extreme compensation occurs (within the effective nonlinear polarization) and supports a field whose transverse E_x and longitudinal E_z components are such that $|E_x| \simeq |E_z|$, i.e., they share the same profile.

The article is organized as follows. In Sec. II we investigate the homogenization of a one-dimensional periodic layered medium comprising both linear (metamaterials) and nonlinear (Kerr media) slabs and we derive the constitutive relations characterizing the effective medium. In Sec. III we focus on the transverse magnetic field configuration and we discuss the effective nonlinear response engineering and the allowed extreme nonlinear regime, together with the transverse power flow reversing effect. In Sec. IV we investigate a class of nonlinear guided waves belonging to the extreme nonlinear regime and we discuss a number of their peculiar properties. The existence of the considered nonlinear guided waves is investigated in Appendix.

II. HOMOGENIZATION OF A 1D NONLINEAR LAYERED MEDIUM

Consider a monochromatic electromagnetic field [whose time dependence is $\exp(-i\omega t)$] propagating through a meta-

material layered medium consisting of periodically repeating, along the y axis, N layers of different media of thicknesses d_j ($j = 1 \dots N$), so that the structure spatial period is $d = \sum_{i=1}^N d_i$ (see Fig. 1 where the case $N = 4$ is depicted). Each one of these N media can be either a linear metamaterial with arbitrary dielectric and magnetic properties or a cubic standard nonlinear medium so the electromagnetic response of the j th medium is modeled by the general constitutive relations

$$\begin{aligned} \mathbf{D}_j &= \epsilon_0 \epsilon_j \mathbf{E}_j + \epsilon_0 \chi_j [(\mathbf{E}_j \cdot \mathbf{E}_j^*) \mathbf{E}_j + \gamma_j (\mathbf{E}_j \cdot \mathbf{E}_j) \mathbf{E}_j^*], \\ \mathbf{B}_j &= \mu_0 \mu_j \mathbf{H}_j, \end{aligned} \quad (1)$$

where ϵ_0 and μ_0 are the vacuum permittivity and permeability constants, whereas \mathbf{E}_j , \mathbf{D}_j , \mathbf{H}_j , \mathbf{B}_j are the complex amplitude of the local electromagnetic field vectors, ϵ_j and μ_j are the relative permittivity and permeability of the j th layer, χ_j and γ_j are the standard parameters characterizing the isotropic cubic nonlinear response of the j th layer [25]. Evidently, $\chi_j = 0$ if the j th layer is filled by a linear medium and $\mu_j = 1$ for a nonlinear dielectric. The linear dielectric constants ϵ_j are here regarded as arbitrary complex numbers since the layers can be filled with lossy and active media. If the field vacuum wavelength is much greater than the spatial period ($\lambda = 2\pi c/\omega \gg d$) the considered periodically nonlinear stratified medium can be homogenized, i.e., its electromagnetic response can be shown to coincide with that of a suitable homogeneous medium. In order to obtain the overall effective response, note that any component of the local electromagnetic field can be assumed, within each layer, independent on y since the layers are extremely small ($d \ll \lambda$). Although this is a very reasonable physical assumption, it can be rigorously proven exploiting the well-known powerful two-scale expansion method [27,28]. Each of the physical observable (macroscopic) electromagnetic field vectors, say \mathbf{V} ($\mathbf{V} = \mathbf{E}, \mathbf{D}, \mathbf{B}, \mathbf{H}$), is obtained by averaging (along the y axis) the layer local fields over the period d , so

$$\mathbf{V} \equiv \langle \mathbf{V}_j \rangle = \sum_{j=1}^N f_j \mathbf{V}_j, \quad (2)$$

where $f_j = d_j/d$ is the volume filling fraction of the j th medium ($\sum_{j=1}^N f_j = 1$) and the averaging has been performed by exploiting the uniformity along y of the local fields \mathbf{V}_j . Within each unit cell (of thickness d), at each plane interface between the j th and $(j+1)$ th layer, the local fields have to satisfy the electromagnetic boundary conditions (continuity of the tangential component of electric and magnetic fields and continuity of the normal components of the displacement and magnetic induction fields) so the local fields are joined by the relations

$$\begin{aligned} E_{jx} &= E_{(j+1)x}, & H_{jx} &= H_{(j+1)x}, \\ E_{jz} &= E_{(j+1)z}, & H_{jz} &= H_{(j+1)z}, \\ D_{jy} &= D_{(j+1)y}, & B_{jy} &= B_{(j+1)y}, \end{aligned} \quad (3)$$

where $j = 1 \dots (N-1)$. Averaging the local fields B_{jx} , B_{jz} and H_{jy} and exploiting the second of Eqs. (1) together with magnetic boundary conditions of Eqs. (3), it is straightforward to prove that the macroscopic fields $\mathbf{B} = \langle \mathbf{B}_j \rangle$ and $\mathbf{H} = \langle \mathbf{H}_j \rangle$

are related by

$$\mathbf{B} = \mu_0 \mu^{(\text{eff})} \mathbf{H}, \quad (4)$$

where the relative magnetic permeability $\mu^{(\text{eff})}$ is the diagonal tensor $\mu^{(\text{eff})} = \text{diag}[\langle \mu_j \rangle, \langle \mu_j^{-1} \rangle^{-1}, \langle \mu_j \rangle]$, which is a very well-established result concerning the homogenization of layered media [29]. As far as the dielectric response is concerned, exploiting the first of Eqs. (1) together with the fact that $E_{jx} = \langle E_{jx} \rangle = E_x$, $E_{jz} = \langle E_{jz} \rangle = E_z$ and $D_{jy} = \langle D_{jy} \rangle = D_y$ [obtained by combining the electric boundary conditions of Eqs. (3) and Eq. (2)] we obtain

$$\begin{aligned} \mathbf{D}_\perp &= \epsilon_0 \langle \epsilon_j \rangle \mathbf{E}_\perp \\ &+ \epsilon_0 [\langle \chi_j \rangle (\mathbf{E}_\perp \cdot \mathbf{E}_\perp^*) \mathbf{E}_\perp + \langle \chi_j \gamma_j \rangle (\mathbf{E}_\perp \cdot \mathbf{E}_\perp) \mathbf{E}_\perp^*] \\ &+ \epsilon_0 [\langle \chi_j | E_{jy} |^2 \rangle \mathbf{E}_\perp + \langle \chi_j \gamma_j E_{jy}^2 \rangle \mathbf{E}_\perp^*], \end{aligned} \quad (5)$$

$$\begin{aligned} D_y &= \epsilon_0 \epsilon_j E_{jy} \\ &+ \epsilon_0 \chi_j [(\mathbf{E}_\perp \cdot \mathbf{E}_\perp^*) E_{jy} + \gamma_j (\mathbf{E}_\perp \cdot \mathbf{E}_\perp) E_{jy}^*] \\ &+ \epsilon_0 \chi_j [(1 + \gamma_j) |E_{jy}|^2 E_{jy}], \end{aligned}$$

where $\mathbf{D}_\perp = D_x \hat{\mathbf{e}}_x + D_z \hat{\mathbf{e}}_z$ and $\mathbf{E}_\perp = E_x \hat{\mathbf{e}}_x + E_z \hat{\mathbf{e}}_z$ are the transverse parts of the macroscopic displacement and electric fields, respectively, and D_y is the y component of the macroscopic displacement field. Note that in the second of Eqs. (6) no averaging has been performed. As a consequence of the layers nonlinear dielectric behavior, the first of Eqs. (6) contains terms where the squares of E_{jy} is suitably averaged. In order to derive the effective medium response, the second of Eqs. (6) has to be solved to express E_{jy} ($j = 1 \dots N$) as a function of the macroscopic fields \mathbf{E}_\perp and D_y . This can be perturbatively done by noting that, since we are considering the standard Kerr effect for each nonlinear layer [25], the terms containing χ_j are much smaller than the term $\epsilon_0 \epsilon_j E_{jy}$ so up to the first order in the field cubic terms, from the second of Eqs. (6), we obtain

$$\begin{aligned} \epsilon_0 E_{jy} &= \frac{1}{\epsilon_j} D_y - \frac{\chi_j}{\epsilon_j^2} [(\mathbf{E}_\perp \cdot \mathbf{E}_\perp^*) D_y + \gamma_j (\mathbf{E}_\perp \cdot \mathbf{E}_\perp) D_y^*] \\ &- \chi_j \frac{1 + \gamma_j}{\epsilon_0 \epsilon_j^4} |D_y|^2 D_y. \end{aligned} \quad (6)$$

Averaging Eq. (6) we obtain a relation joining the macroscopic field E_y and the fields \mathbf{E}_\perp and D_y so this relation, if its nonlinear contributions are much smaller than the leading linear term, can be inverted to perturbatively yield D_y as a function of \mathbf{E}_\perp and E_y . Therefore, up to the first order in the field cubic terms, we obtain

$$\begin{aligned} D_y &= \epsilon_0 \langle \epsilon_j^{-1} \rangle^{-1} E_y \\ &+ \epsilon_0 \left[\frac{\langle \chi_j \epsilon_j^{-2} \rangle}{\langle \epsilon_j^{-1} \rangle^2} \mathbf{E}_\perp \cdot \mathbf{E}_\perp^* + \frac{\langle \chi_j (1 + \gamma_j) \epsilon_j^{-4} \rangle}{2 \langle \epsilon_j^{-1} \rangle^4} |E_y|^2 \right] E_y \\ &+ \epsilon_0 \left[\frac{\langle \chi_j \gamma_j \epsilon_j^{-2} \rangle}{\langle \epsilon_j^{-1} \rangle^2} \mathbf{E}_\perp \cdot \mathbf{E}_\perp + \frac{\langle \chi_j (1 + \gamma_j) \epsilon_j^{-4} \rangle}{2 \langle \epsilon_j^{-1} \rangle^4} E_y^2 \right] E_y^*. \end{aligned} \quad (7)$$

Substituting the fields E_{jy} of Eqs. (6) into the first of Eqs. (6) and using Eq. (7) (neglecting everywhere the terms containing powers of χ_j higher than one) we obtain

$$\begin{aligned} \mathbf{D}_\perp &= \epsilon_0 \langle \epsilon_j \rangle \mathbf{E}_\perp \\ &+ \epsilon_0 \left[\langle \chi_j \rangle \mathbf{E}_\perp \cdot \mathbf{E}_\perp^* + \frac{\langle \chi_j \epsilon_j^{-2} \rangle}{\langle \epsilon_j^{-1} \rangle^2} |E_y|^2 \right] \mathbf{E}_\perp \\ &+ \epsilon_0 \left[\langle \chi_j \gamma_j \rangle \mathbf{E}_\perp \cdot \mathbf{E}_\perp + \frac{\langle \chi_j \gamma_j \epsilon_j^{-2} \rangle}{\langle \epsilon_j^{-1} \rangle^2} E_y^2 \right] \mathbf{E}_\perp^*. \end{aligned} \quad (8)$$

Equations (7) and (8) are the constitutive dielectric relations characterizing the effective medium obtained by the homogenization of the considered 1D layered medium since they solely contain the macroscopic fields. Equations (7) and (8) can be written as

$$\begin{pmatrix} D_x \\ D_y \\ D_z \end{pmatrix} = \epsilon_0 \begin{pmatrix} \epsilon_{xx}^{(\text{eff})} & \epsilon_{xy}^{(\text{eff})} \epsilon_{xz}^{(\text{eff})} \\ \epsilon_{yx}^{(\text{eff})} & \epsilon_{yy}^{(\text{eff})} \epsilon_{yz}^{(\text{eff})} \\ \epsilon_{zx}^{(\text{eff})} & \epsilon_{zy}^{(\text{eff})} \epsilon_{zz}^{(\text{eff})} \end{pmatrix} \begin{pmatrix} E_x \\ E_y \\ E_z \end{pmatrix}, \quad (9)$$

where the components of the effective nonlinear permittivity tensor $\epsilon^{(\text{eff})}$ are

$$\begin{aligned} \epsilon_{xx}^{(\text{eff})} &= \langle \epsilon_j \rangle + (\langle \chi_j \rangle + \langle \chi_j \gamma_j \rangle) |E_x|^2 + \frac{\langle \chi_j \epsilon_j^{-2} \rangle}{\langle \epsilon_j^{-1} \rangle^2} |E_y|^2 \\ &+ \langle \chi_j \rangle |E_z|^2, \\ \epsilon_{yy}^{(\text{eff})} &= \langle \epsilon_j^{-1} \rangle^{-1} + \frac{\langle \chi_j \epsilon_j^{-2} \rangle}{\langle \epsilon_j^{-1} \rangle^2} |E_x|^2 + \frac{\langle \chi_j \epsilon_j^{-4} (1 + \gamma_j) \rangle}{\langle \epsilon_j^{-1} \rangle^4} |E_y|^2 \\ &+ \frac{\langle \chi_j \epsilon_j^{-2} \rangle}{\langle \epsilon_j^{-1} \rangle^2} |E_z|^2, \\ \epsilon_{zz}^{(\text{eff})} &= \langle \epsilon_j \rangle + \langle \chi_j \rangle |E_x|^2 + \frac{\langle \chi_j \epsilon_j^{-2} \rangle}{\langle \epsilon_j^{-1} \rangle^2} |E_y|^2 \\ &+ (\langle \chi_j \rangle + \langle \chi_j \gamma_j \rangle) |E_z|^2, \\ \epsilon_{xy}^{(\text{eff})} &= \frac{\langle \chi_j \gamma_j \epsilon_j^{-2} \rangle}{\langle \epsilon_j^{-1} \rangle^2} E_x^* E_y, \\ \epsilon_{yx}^{(\text{eff})} &= \frac{\langle \chi_j \gamma_j \epsilon_j^{-2} \rangle}{\langle \epsilon_j^{-1} \rangle^2} E_x E_y^*, \\ \epsilon_{xz}^{(\text{eff})} &= \langle \chi_j \gamma_j \rangle E_x^* E_z, \\ \epsilon_{zx}^{(\text{eff})} &= \langle \chi_j \gamma_j \rangle E_x E_z^*, \\ \epsilon_{yz}^{(\text{eff})} &= \frac{\langle \chi_j \gamma_j \epsilon_j^{-2} \rangle}{\langle \epsilon_j^{-1} \rangle^2} E_y^* E_z, \\ \epsilon_{zy}^{(\text{eff})} &= \frac{\langle \chi_j \gamma_j \epsilon_j^{-2} \rangle}{\langle \epsilon_j^{-1} \rangle^2} E_y E_z^*, \end{aligned} \quad (10)$$

From Eq. (9) we note that the effective medium behaves like an anisotropic Kerr medium whose nonlinear properties can be tailored by suitably choosing the underlying layered composite. Note that, in the specific case of linear layers (i.e., $\chi_j = 0$ for all j), the effective permittivity reduces to the diagonal tensor $\epsilon_{\text{eff}} = \text{diag}[\langle \epsilon_j \rangle, \langle \epsilon_j^{-1} \rangle^{-1}, \langle \epsilon_j \rangle]$, reproducing

a well-known result concerning homogenization of linear layered media [29–31].

III. EXTREME ELECTRODYNAMICS OF TM FIELDS

Electromagnetic propagation through the homogenized medium of Sec. II is described by the macroscopic Maxwell equations

$$\begin{aligned}\nabla \times \mathbf{E} &= i\omega\mathbf{B}, \\ \nabla \times \mathbf{H} &= -i\omega\mathbf{D}\end{aligned}\quad (11)$$

and the constitutive relations of Eqs. (4), (7), and (8). Hereafter, we focus on transverse magnetic (TM) electromagnetic fields (see Fig. 1) of the form

$$\begin{aligned}\mathbf{E} &= E_x(x,z)\hat{\mathbf{e}}_x + E_z(x,z)\hat{\mathbf{e}}_z, \\ \mathbf{H} &= H_y(x,z)\hat{\mathbf{e}}_y.\end{aligned}\quad (12)$$

Substituting the field of Eqs. (12) into Eqs. (9) and (4) we obtain

$$\begin{aligned}\mathbf{D} &= \epsilon_0\epsilon\mathbf{E} + \epsilon_0\chi[(\mathbf{E} \cdot \mathbf{E}^*)\mathbf{E} + \gamma(\mathbf{E} \cdot \mathbf{E})\mathbf{E}^*], \\ \mathbf{B} &= \mu_0\mu\mathbf{H},\end{aligned}\quad (13)$$

where $\mathbf{D} = D_x(x,z)\hat{\mathbf{e}}_x + D_z(x,z)\hat{\mathbf{e}}_z$, $\mathbf{B} = B_y(x,z)\hat{\mathbf{e}}_y$, and the effective parameters

$$\begin{aligned}\epsilon &= \sum_{j=1}^N f_j \epsilon_j, & \mu &= \left[\sum_{j=1}^N f_j \mu_j^{-1} \right]^{-1}, \\ \chi &= \sum_{j=1}^N f_j \chi_j, & \gamma &= \frac{1}{\chi} \sum_{j=1}^N f_j \chi_j \gamma_j.\end{aligned}\quad (14)$$

The parameters ϵ , χ , and γ of Eqs. (14) are easily deduced by Eqs. (10) by setting $E_y = 0$, whereas the parameter μ of Eqs. (14) is simply the yy component of the relative magnetic permeability $\mu^{(\text{eff})}$ of Eq. (4). Therefore the effective dielectric response experienced by a TM field coincides with the standard isotropic Kerr response. Analogously to what happens in linear layered media, we note, from Eqs. (14), that the permittivity ϵ and the permeability μ are the weighted and harmonic weighted means, respectively, so the former is bounded by the minimum and maximum of its microscopic values, whereas the latter is unbounded since some μ_j can

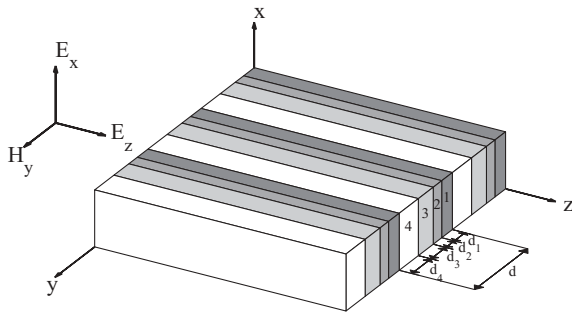


FIG. 1. Geometry of the nonlinear layered composite and TM electromagnetic field configuration.

be negative. It is worth stressing that the averaging of the microscopic linear parameters additionally allows an efficient loss management since, combining lossy and gain media, one can design an effective medium whose effective parameters ϵ and μ have negligible imaginary parts [32]. On the other hand, χ is the weighted mean of the constituents nonlinear Kerr coefficients and this is in agreement with the results of Ref. [33–35]. More interestingly, γ is generally not the weighted mean of its microscopic values since some χ_j can be negative (corresponding to defocusing nonlinear layers), so γ can assume any positive and negative value. This result is particularly interesting since, for standard cubic isotropic materials, there is, in general, a small number of available γ (depending on the physical mechanism supporting the nonlinear response [25]), whereas, for composite materials, it has been shown in Ref. [22] that γ can span the whole range $0 < \gamma < 3$.

Even though Eqs. (13) formally coincide with the standard isotropic Kerr response, the considered layered material can support a nonlinear electromagnetic phenomenology that differs substantially from that observed in a standard Kerr medium, as discussed in the following three subsections.

A. Extreme nonlinear regime

Consider a layered medium for which ϵ is such that $0 < \text{Re}(\epsilon) \ll 1$, $|\text{Im}(\epsilon)| \ll \text{Re}(\epsilon)$ and the effective nonlinear coefficient χ is of the same order of magnitude of underlying coefficients χ_j (i.e., $|\chi| \sim |\chi_j|$). An effective dielectric permittivity with a very small real part and a negligible imaginary part can be achieved by combining positive and negative standard dielectric layers ($|\text{Re}(\epsilon_j)| > 1$) together with gain media (generally unavoidable since absorption due to negative dielectrics can not be in principle neglected [32]). For the sake of simplicity let us consider the case $\gamma = 0$. If the electromagnetic field propagating through the medium is such that

$$|E_x|^2 + |E_z|^2 \sim \left| \frac{\epsilon}{\chi} \right|, \quad (15)$$

we have $|\chi_j(\mathbf{E} \cdot \mathbf{E}^*)| \sim |\epsilon| \ll |\epsilon_j|$ so, in the first of Eqs. (1), the nonlinear part is much smaller than the linear contribution $\epsilon_0\epsilon_j\mathbf{E}_j$. Therefore, the nonlinear layers are in the presence of a field whose intensity is sufficiently small for their response to be purely cubic and, as a consequence, the microscopic responses of Eqs. (1) hold and the macroscopic constitutive relation in the first of Eqs. (13), holds as well. On the other hand, combining Eq. (15) and the first of Eq. (13) we conclude that, as opposed to what happens in standard nonlinear materials, the considered layered medium is able to support the extreme nonlinear regime where the electromagnetic field is such that the linear contribution $\epsilon\mathbf{E}$ and the nonlinear term $\chi(\mathbf{E} \cdot \mathbf{E}^*)\mathbf{E}$ in the overall dielectric response have the same order of magnitude. It is evident that the same argument, with some slight changes, allows to prove that the extreme nonlinear regime is observable for any value of γ . Even though the advantages of such an extreme nonlinear regime are self-evident, it is worthwhile to compare it to the standard paraxial nonlinear optical situation where the overall refractive index is $n_0 + \delta n$, where n_0 is the background linear refractive

index and $\delta n = n_2 I \ll n_0$ is the Kerr nonlinear term (where I is the optical intensity). In this situation the field satisfies the equation

$$\nabla^2 \mathbf{E} + k_0^2 (n_0^2 + 2n_0 \delta n) \mathbf{E} = 0 \quad (16)$$

($k_0 = \omega/c$) and, within the paraxial regime, the field is of the form $\mathbf{E} = e^{ikz} \mathbf{A}$. At this point one chooses $k = k_0 n_0$ since, substituting the paraxial field into Eq. (16) the term $k_0^2 n_0^2 \mathbf{E}$ (responsible for the fast spatial variation of the field) is removed and the paraxial equation $i \frac{\partial \mathbf{A}}{\partial z} + \frac{1}{2k} \nabla_{\perp}^2 \mathbf{A} = -\frac{k}{n_0} \delta n \mathbf{A}$ is readily obtained by neglecting the term containing $\frac{\partial^2 \mathbf{A}}{\partial z^2}$. Therefore, in standard paraxial nonlinear optics, δn can play an important role in Eq. (16) since the large linear contribution proportional to n_0^2 is suppressed by the presence of the carrier plane wave. In other words, the nonlinear Kerr contribution $\epsilon_0 \chi |\mathbf{E}|^2 \mathbf{E}$ is not requested to compete against the whole linear part, $\epsilon_0 \epsilon \mathbf{E}$, of the dielectric response. However, in the case of the extreme nonlinear regime discussed in this section, this competition can happen and therefore the nonlinearity is not confined to solely drive the slowly varying amplitude \mathbf{A} .

B. Transverse power flow reversing

The extreme nonlinear regime can support propagation of beams characterized by exotic properties such as the reversing of the electromagnetic power flow along the beam transverse profile [26]. In order to discuss this phenomenon, consider a TM field describing a beam mainly propagating along the z axis, i.e., a field of the form $H_y(x, z) = e^{iKz} A(x, z)$ with the requirement $|\partial_z A| \ll K|A|$ (K being a wave vector depending on the actual electromagnetic configuration). In this case Maxwell equations of Eqs. (11) yield

$$H_y = \frac{\omega}{K} D_x, \quad (17)$$

$$H_y = \frac{1}{\omega \mu_0 \mu} \left(K E_x + i \frac{\partial E_z}{\partial x} \right),$$

where it has been assumed that $\partial_z H_y \simeq iK H_y$ and $\partial_z E_x \simeq iK E_x$. Exploiting Eqs. (17), the z component of the time-averaged Poynting vector $S_z = (1/2) \text{Re}(H_y E_x^*)$ can be expressed through the equivalent relations

$$S_z = \frac{\omega}{2K} \text{Re}(D_x E_x^*) \quad (18)$$

$$S_z = \frac{1}{2\omega \mu_0 \mu} \text{Re} \left[\left(K E_x + i \frac{\partial E_z}{\partial x} \right) E_x^* \right].$$

If, for example, $\epsilon > 0$, $\mu > 0$, $\chi < 0$, and $\gamma = 0$, for an electromagnetic beam whose peak electric field strength is greater than $\sqrt{|\epsilon/\chi|}$ (extreme nonlinear regime), it is evident from the first of Eqs. (13) that D_x and E_x are antiparallel around the propagation axis (i.e., where $|\chi(\mathbf{E} \cdot \mathbf{E}^*)| > \epsilon$) and parallel elsewhere so that, from the first of Eqs. (18), S_z is negative near the beam axis and positive elsewhere. In other words the beam is characterized by a power flow whose direction reverses its sign along the transverse profile and this is due to sign flipping of D_x along the wave transverse profile while E_x does not change its sign. Note that the sign flipping of D_x corresponds to a sign flipping of H_y [see the first of Eqs. (17)] so, considering the second of Eqs. (17),

this can happen without sign flipping of E_x only if $\partial E_z / \partial x$ is not negligible with respect $K E_x$. Therefore power flow reversing can take place only if the field has a transverse size comparable with $1/K$. It is worth stressing that the discussed power flow reversing differs from the effect that, in left-handed metamaterials, the Poynting vector is antiparallel to the carrier wave vector which is a consequence of the fact that, in such media, $\epsilon < 0$ and $\mu < 0$ (with $n < 0$). On the other hand, in our case, $\mu > 0$ and the sign of the power flow is not uniform being controlled by the field intensity through the nonlinearity.

C. Linear and nonlinear parameters design

In order to discuss the impact of the wide ranges of the parameters of Eqs. (14), made possible by linear and nonlinear design, on electromagnetic phenomenology, we consider the situation where the effective dielectric permittivity ϵ and magnetic permeability μ are real, so, after substituting the expression for the TM field of Eqs. (12) into Eqs. (11), eliminating the magnetic field and using Eqs. (13) we get

$$\frac{\partial^2 U_z}{\partial \xi \partial \zeta} - \frac{\partial^2 U_x}{\partial \zeta^2} = \sigma_\epsilon \sigma_\mu U_x + \sigma_\mu [(1 + \gamma) |U_x|^2 U_x + (U_x U_z^* + \gamma U_x^* U_z) U_z], \quad (19)$$

$$\frac{\partial^2 U_x}{\partial \xi \partial \zeta} - \frac{\partial^2 U_z}{\partial \xi^2} = \sigma_\epsilon \sigma_\mu U_z + \sigma_\mu [(1 + \gamma) |U_z|^2 U_z + (U_z U_x^* + \gamma U_z^* U_x) U_x],$$

where dimensionless variables and fields have been introduced according to

$$x = \frac{1}{\sqrt{|\epsilon \mu|} k_0} \xi, \quad z = \frac{1}{\sqrt{|\epsilon \mu|} k_0} \zeta, \quad (20)$$

$$U_x = \sqrt{\left| \frac{\chi}{\epsilon} \right|} E_x, \quad U_z = \sqrt{\left| \frac{\chi}{\epsilon} \right|} E_z,$$

and $k_0 = \omega/c$, whereas $\sigma_\epsilon = \text{sgn}(\epsilon \chi)$ and $\sigma_\mu = \text{sgn}(\mu \chi)$ are the signs of the products $\epsilon \chi$ and $\mu \chi$, respectively. As opposed to the linear regime where electric field behavior solely depends on the sign of $\epsilon \mu$ [1], from Eqs. (19) we note that, in the present approach, the nonlinear dynamics separately depends on the signs of $\epsilon \chi$ and $\mu \chi$, i.e., the presence of the nonlinearity breaks the symmetry between the roles played by the signs of ϵ and μ [36,37]. From Eqs. (20) we note that ϵ , μ , and χ scale the actual physical size and amplitude of the field so, since the effective parameters can in principle be independently chosen [see Eqs. (14)], for each solution of Eqs. (19), a suitable layered medium can be designed in such a way that the actual electromagnetic field has a prescribed geometrical size and intensity [see Eqs. (20)]. As an example, in the case of beam propagation, such an electromagnetic scaling freedom can allow to observe nonparaxial feature of a beam whose transverse width is much greater than the vacuum wavelength (if $|\epsilon \mu| \ll 1$) or, on the contrary, to observe the standard paraxial phenomenology for beams whose transverse width is much smaller than the vacuum wavelength (if $|\epsilon \mu| \gg 1$) and, remarkably, this can be done by avoiding any unfeasible requirement on the intensity.

The parameter γ plays a role that differs fundamentally since it cannot be generally removed from Eqs. (19)

with a field transformation. Setting $U_x = A_x e^{i\phi_x}$ and $U_z = A_z e^{i\phi_z}$ (where A_x , A_z , ϕ_x , and ϕ_z are real), the nonlinear terms of Eqs. (19), namely $N_x = (1 + \gamma)|U_x|^2 U_x + (U_x U_z^* + \gamma U_x^* U_z) U_z$ and $N_z = (1 + \gamma)|U_z|^2 U_z + (U_z U_x^* + \gamma U_z^* U_x) U_x$, can be written as

$$\begin{aligned} N_x &= [(1 + \gamma)A_x^2 + (1 + \gamma e^{-2i(\phi_x - \phi_z)})A_z^2] A_x e^{i\phi_x}, \\ N_z &= [(1 + \gamma e^{2i(\phi_x - \phi_z)})A_x^2 + (1 + \gamma)A_z^2] A_z e^{i\phi_z}, \end{aligned} \quad (21)$$

from which we note that γ is responsible for a nonlinear coupling between the two field components which is highly sensitive to the phase difference $\phi_x - \phi_z$. The case $\gamma = -1$ is particularly interesting since in Eqs. (21) the terms proportional to $(1 + \gamma)$ vanish so that each field component is nonlinearly driven only by the other component and such coupling is fully sensitive the phase difference. Also intriguing is the regime $|\gamma| \gg 1$ since two major opposite situations exist. If the phases of U_x and U_z are equal, from Eqs. (21) it is evident that the overall nonlinear polarization is proportional to $(1 + \gamma)$ so that, if $|\gamma| \gg 1$, the effective nonlinear response can be enhanced. If, on the other hand, the phase difference between U_x and U_z is $\pi/2$, the overall nonlinear response of Eqs. (21) solely contains the terms $(A_x^2 + A_z^2)$ and $\gamma(A_x^2 - A_z^2)$, so, if $|\gamma| \gg 1$ (for realistic bounded fields), the compensation $A_x^2 \sim A_z^2$ has to occur in order to prevent the divergence of the term proportional to γ in Eqs. (19).

IV. NONLINEAR GUIDED WAVES

As explained in the above section, the nonlinear response of the proposed Kerr metamaterial is easy to manage and, since the accesible ranges of its parameters are very wide, one can devise situations where the medium supports a nonlinear electrodynamic phenomenology. In order to probe the regime, we consider here a class of fields which are sufficiently simple to allow a full analytical treatment and, at the same time, rigged with enough structure to show many of the effects. More specifically, we consider nonlinear guided waves propagating along the z axis of the form

$$\begin{aligned} U_x(\xi, \zeta) &= e^{i\beta\zeta} u_x(\xi), \\ U_z(\xi, \zeta) &= e^{i\beta\zeta} i u_z(\xi), \end{aligned} \quad (22)$$

where β is a real constant and the amplitudes u_x and u_z are real. Substituting the field of Eqs. (22) into Eqs. (19) we obtain

$$\begin{aligned} -\beta \frac{du_z}{d\xi} + \beta^2 u_x &= \sigma_\mu [\sigma_\epsilon + \Psi_x] u_x, \\ \beta \frac{du_x}{d\xi} - \frac{d^2 u_z}{d\xi^2} &= \sigma_\mu [\sigma_\epsilon + \Psi_z] u_z, \end{aligned} \quad (23)$$

where

$$\begin{aligned} \Psi_x(\xi) &= (1 + \gamma)u_x^2(\xi) + (1 - \gamma)u_z^2(\xi), \\ \Psi_z(\xi) &= (1 - \gamma)u_x^2(\xi) + (1 + \gamma)u_z^2(\xi). \end{aligned} \quad (24)$$

Using Eqs. (24), it is worth noting that, from the first of Eqs. (13), the vector \mathbf{D} can be expressed as

$$\begin{aligned} D_x &= \epsilon_0 \chi \sqrt{\left| \frac{\epsilon}{\chi} \right|^3} (\sigma_\epsilon + \Psi_x) u_x e^{i\beta\zeta}, \\ D_z &= \epsilon_0 \chi \sqrt{\left| \frac{\epsilon}{\chi} \right|^3} (\sigma_\epsilon + \Psi_z) i u_z e^{i\beta\zeta}, \end{aligned} \quad (25)$$

from which we note that

$$\begin{aligned} \epsilon_x^{(NL)} &= |\epsilon| \text{sgn}(\chi) (\sigma_\epsilon + \Psi_x) \\ \epsilon_z^{(NL)} &= |\epsilon| \text{sgn}(\chi) (\sigma_\epsilon + \Psi_z) \end{aligned} \quad (26)$$

act, for the fields of Eqs. (22), as effective nonlinear dielectric permittivity. The quantities of Eqs. (24) play a fundamental role in our discussion since it is evident that, if the conditions $|\Psi_x| \ll 1$ and $|\Psi_z| \ll 1$ do not hold along the profile of a nonlinear guided wave, the linear and nonlinear contribution in Eq. (25) are comparable, i.e., the considered nonlinear guided wave belongs to the extreme nonlinear regime we have discussed in Sec. III A.

We consider solutions of Eqs. (23) with definite parity where u_x and u_z are spatially even [$u_x(\xi) = u_x(-\xi)$] and odd [$u_z(\xi) = -u_z(-\xi)$], respectively, and, as a consequence, we adopt the boundary conditions

$$\begin{aligned} u_x(0) &= u_{x0}, & u_z(0) &= 0, \\ u_x(+\infty) &= u_{x\infty}, & u_z(+\infty) &= u_{z\infty}. \end{aligned} \quad (27)$$

It is worth stressing that, due to the feasible possibility of arbitrary choosing the effective linear and nonlinear parameters characterizing the effective nonlinear medium, we consider here solutions of Eqs. (23) and (27) for $\sigma_\epsilon = \pm 1$, $\sigma_\mu = \pm 1$, and, remarkably, for any real γ . In the appendix we show that the system of Eqs. (23) is integrable and we derive the existence conditions characterizing the nonlinear guided waves satisfying Eqs. (27), i.e, for each possible combinations of σ_ϵ and σ_μ , we derive a γ -dependent range of $u_{x\infty}^2$ [i.e., $u_{\min}^2(\gamma) < u_{x\infty}^2 < u_{\max}^2(\gamma)$] corresponding to nonlinear waves existence. The resulting phenomenology is reported in Table I. For each obtained nonlinear guided wave the propagation constant β and the asymptotical value $u_{z\infty}$ are given by (see the appendix)

$$\begin{aligned} \beta^2 &= \frac{2\gamma\sigma_\mu}{1 + \gamma} (\sigma_\epsilon + 2u_{x\infty}^2) = \sigma_\mu [\sigma_\epsilon + \Psi_x(+\infty)], \\ u_{z\infty}^2 &= \frac{-\sigma_\epsilon - (1 - \gamma)u_{x\infty}^2}{1 + \gamma}, \end{aligned} \quad (28)$$

where the second expression for β is obtained from the first by exploiting the first of Eqs. (24). It is worth noting that, for each $u_{x\infty}$, these values of β and $u_{z\infty}$ are obtained by requiring that the nonlinear guided wave is asymptotically spatially uniform (i.e., by annulling the derivatives in Eqs. (23) for $\xi \rightarrow \infty$) and, exploiting Eqs. (26), this implies that

$$\begin{aligned} \epsilon_x^{(NL)}(+\infty) &= \frac{|\epsilon\mu|}{\mu} \beta^2, \\ \epsilon_z^{(NL)}(+\infty) &= 0. \end{aligned} \quad (29)$$

TABLE I. Guided waves existence ranges of $u_{x\infty}^2$ depending on γ , σ_ϵ , and σ_μ .

	$\sigma_\epsilon = -1$ $\sigma_\mu = 1$	$\sigma_\epsilon = -1$ $\sigma_\mu = -1$
$\gamma > 0$		$\frac{\gamma}{\gamma^2+4\gamma+1} < u_{x\infty}^2 < \frac{1}{2}$
$-1 < \gamma < 0$	$u_{x\infty}^2 < \frac{1}{2}$	
$\gamma < -1$		$\frac{1}{1-\gamma} < u_{x\infty}^2 < \frac{1}{2}$

From a physical point of view, the second of Eqs. (29) states that the considered nonlinear waves can propagate through the medium only if, asymptotically, the nonlinear term exactly balances the linear one to yield an overall vanishing dielectric constant, i.e.,

$$\Psi_z(+\infty) = -\sigma_\epsilon. \quad (30)$$

This proves that the nonlinear guided waves we are considering always belong to the extreme nonlinear regime, i.e., they cannot be observed in standard Kerr media. It is worth stressing that the subfamily of nonlinear guided waves with $u_{z\infty} = 0$ do not require such an asymptotical compensation mechanisms since, for $\xi \rightarrow \infty$, the second of Eqs. (23) vanishes together with $u_{z\infty}$. To sum up, an asymptotically spatially uniform wave can exist only if $D_z(\infty) = 0$ (since $\partial_x H_y = -i\omega D_z$) and this can be achieved by requiring either $u_{z\infty} = 0$ or $\epsilon_z^{(NL)}(+\infty) = 0$, the second situation being investigated in the present article.

Since the waves we are investigating always belong to the extreme nonlinear regime, power flow reversing discussed in Sec. III B is expected. For the field of Eqs. (22), the time-averaged Poynting vector $\mathbf{S} = (1/2)\text{Re}[\mathbf{E} \times \mathbf{H}^*]$ is given by

$$\begin{aligned} \mathbf{S} &= S_0 \text{sgn}(\mu) \left[\left(\beta u_x - \frac{du_z}{d\xi} \right) u_x \right] \hat{\mathbf{e}}_z, \\ \mathbf{S} &= S_0 \frac{\text{sgn}(\chi)}{\beta} (\sigma_\epsilon + \Psi_x) u_x^2 \hat{\mathbf{e}}_z, \end{aligned} \quad (31)$$

where $S_0 = \sqrt{(\epsilon_0 |\epsilon|^3) / (4\mu_0 |\mu| |\chi|^2)}$ and the second expression is obtained from the first one by exploiting the first of Eqs. (23) to eliminate the derivative of u_z and the first of Eqs. (24). Note that Eqs. (31) coincide with Eqs. (18) (with the identification $K = \sqrt{|\epsilon\mu|k_0\beta}$), the difference lying in the fact that, for the nonlinear guided waves we are considering, Eqs. (31) are exact due to the waves propagation invariance.

A. Nonlinear guided waves for $\sigma_\epsilon = -1$ and $\sigma_\mu = 1$

The situation $\sigma_\epsilon = -1$ and $\sigma_\mu = 1$ is very intriguing since $\text{sgn}(\epsilon\mu) = \sigma_\epsilon\sigma_\mu = -1$ and, therefore, in the absence of nonlinearity, no propagation can occur since the medium can support only evanescent waves. On the contrary, we have shown that, in this situation (see first column of Table I), the nonlinear Kerr metamaterial can support propagating nonlinear guided waves (i.e., with real propagation constant β). In order to grasp this fact, we note, from the first of Eqs. (28), for $\sigma_\epsilon = -1$ and $\sigma_\mu = 1$, we obtain

$$\beta^2 = -1 + \Psi_x(+\infty), \quad (32)$$

from which it is evident that, in the absence of the nonlinearity, $\beta^2 = -1$, i.e., only evanescent waves exist. However, combining the first of Eqs. (24) and the second of Eqs. (28), we obtain

$$\Psi_x(+\infty) = 1 - \frac{2\gamma}{1+\gamma} (1 - 2u_{x\infty}^2), \quad (33)$$

from which it is evident that, for $-1 < \gamma < 0$ and $u_{x\infty}^2 < 1/2$ (see the first column of Table I), $\Psi_x(+\infty) > 1$ so $\beta^2 > 0$ and the nonlinear wave can propagate through the medium. From a physical point of view, the same result can be understood by regarding the nonlinear guided wave as a background infinite plane wave with a distortion around $\xi = 0$. The background nonlinear plane wave can propagate through the medium since its amplitude is such that $\Psi_x(+\infty) > 1$ so that the effective nonlinear dielectric permittivity in the first of Eqs. (26) is such that $\mu\epsilon_x^{(NL)} = |\epsilon\mu|[-1 + \Psi_x(+\infty)] > 0$. In other words, in the extreme nonlinear regime, the nonlinear polarizability overcomes the linear dielectric contribution in such a way that the sign of the effective overall dielectric permittivity is opposed to that of the linear dielectric permittivity and the waves are consistently not evanescent.

In Fig. 2 we plot various profiles of $u_x(\xi)$ and $u_z(\xi)$ for $\gamma = -1/2$ and for $u_{x\infty}^2 < 1/2$. In Fig. 3 we plot the profiles of $u_x(\xi)$ and $u_z(\xi)$ for different nonlinear guided waves, in the range $-0.8 < \gamma < -0.1$, each characterized by the same asymptotical value $u_{x\infty} = \sqrt{0.4}$. As explained in the appendix, more than one nonlinear guided wave (for a given γ) can be generally found for each $u_{x\infty}$ and, in the situation of Fig. 3, there are specifically two waves, the first being reported in Figs. 3(a) and 3(b) and the second in Figs. 3(c) and 3(d). The most striking feature emerging from Fig. 3 is that, for a given $u_{x\infty}$ the closer γ to -1 , the sharper the profile of u_x , i.e., γ produces a hyperfocusing effect for this waves when it approaches the value $\gamma = -1$. As expected (see the discussion of Sec. III C), the situation $\gamma = -1$ is

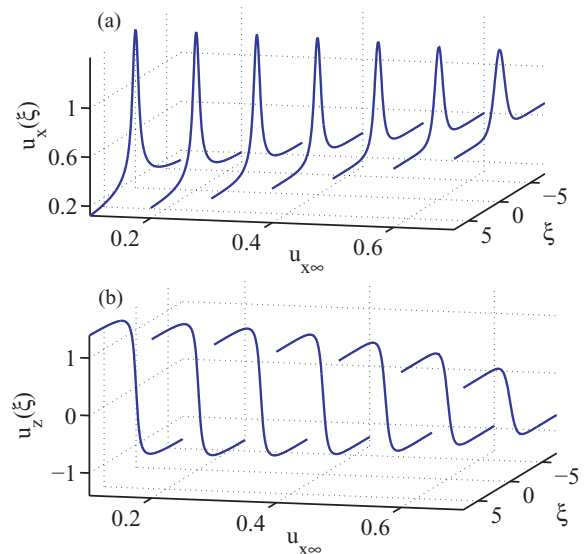


FIG. 2. (Color online) Nonlinear guided waves transverse profile of (a) $u_x(\xi)$ and (b) $u_z(\xi)$ at different values of $u_{x\infty}$ for $\sigma_\epsilon = -1$, $\sigma_\mu = 1$, $\gamma = -1/2$.

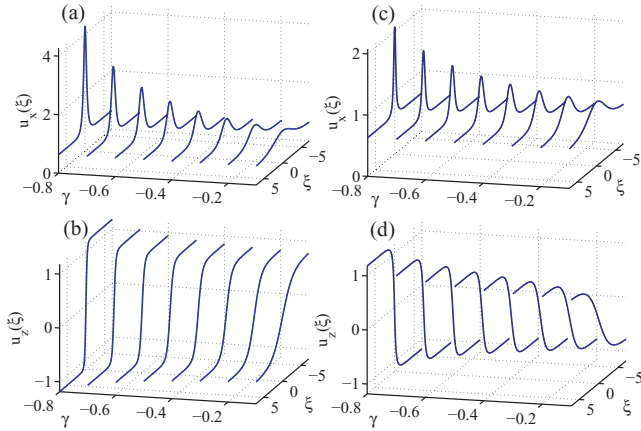


FIG. 3. (Color online) Profiles of u_x and u_z of various nonlinear guided waves with $\sigma_\epsilon = -1$ and $\sigma_\mu = 1$ and with γ spanning the range $-0.8 < \gamma < -0.1$. All the waves are characterized by the same asymptotical value $u_{x\infty} = \sqrt{0.4}$. For each γ two waves exist, the first shown in Figs. 3(a) and 3(b) and the second in Figs. 3(c) and 3(d).

peculiar, displaying a phenomenology absent for other values of γ . From a physical point of view, the hyperfocusing effect results from the combination of two different mechanisms. For the first one, we note that, since $\epsilon_z^{(NL)}(+\infty) = 0$ [see the second of Eqs. (29)], if γ is very close to -1 , from the second of Eqs. (26) and the second of Eqs. (24), we conclude that $u_{z\infty}$ is much greater than 1 [in agreement with the second of Eqs. (28) evaluated for $\gamma \simeq -1$]. Therefore, $|u_z(\xi)|$ is much greater than 1 everywhere apart from a small region around $\xi = 0$ where u_z is very small [since $u_z(0) = 0$] and $du_z/d\xi$ is very large. The second mechanism supporting hyperfocusing is based on the fact that, for $\gamma \simeq -1$, the field x component (u_x) is nonlinearly driven solely by u_z (see the discussion of Sec. III C). Therefore, in the region where u_z is very small and $du_z/d\xi$ is very large, from the first of Eqs. (23), it is evident that $u_x(\xi)$ displays a very pronounced peak, i.e., u_x is tightly squeezed by u_z for $\gamma \simeq -1$. In Fig. 4 we report the z component of the normalized Poynting vector S_z/S_0 [see Eqs. (31)] evaluated for the waves reported in Fig. 3. Note that the above-discussed hyperfocusing effectively corresponds to a tight energy localization around $\xi = 0$ for γ close to -1 . This effect is particularly evident from the inset of Fig. 4(a) where we plot the peak width Δ of S_z/S_0 as a function of γ . The power flows reported in Fig. 4(b) clearly displays the transverse power flow reversing discussed in Sec. III B since there is a region around $\xi = 0$ where $S_z/S_0 < 0$, whereas $S_z/S_0 > 0$ elsewhere. Note that the power flows reported in Fig. 4(a) does not exhibit transverse power flow reversing and this can be easily understood considering the structures of the two waves reported in Fig. 3. The z component of the first wave is such that $du_z/d\xi < 0$ [see Fig. 3(b)] so, from the first of Eq. (31), the two bell-shaped contributions u_x^2 and $-u_x du_z/d\xi$ are both positive, yielding the $S_z/S_0 > 0$. On the other hand, the second wave is such that $du_z/d\xi > 0$ [see Fig. 3(d)] and, therefore, in the first of Eqs. (31), the two contributions have different signs and S_z/S_0 can flip its sign along the transverse profile.

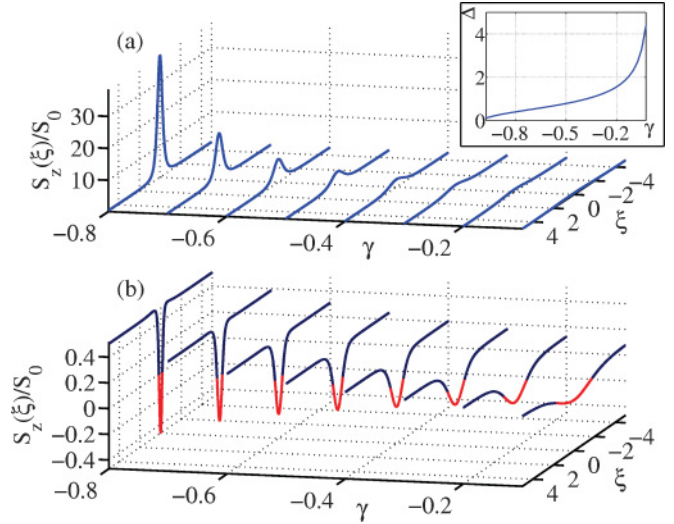


FIG. 4. (Color online) Profile of the normalized Poynting vector z component S_z/S_0 evaluated for the nonlinear guided waves of Fig. 3. Here $\text{sgn}(\epsilon) = -1$, $\text{sgn}(\mu) = 1$, and $\text{sgn}(\chi) = 1$. (a) S_z/S_0 evaluated for the waves reported in Figs. 3(a) and 3(b). (b) S_z/S_0 evaluated for the waves reported in Figs. 3(c) and 3(d). In the inset of (a), the width Δ (root-mean-square deviation) of the various S_z/S_0 reported in (a) is plotted as a function of γ .

B. Nonlinear guided waves for $\sigma_\epsilon = -1$ and $\sigma_\mu = -1$

For $\sigma_\epsilon = -1$ and $\sigma_\mu = -1$, waves are allowed to propagate in the linear regime and the nonlinear guided waves can propagate if

$$\beta^2 = 1 - \Psi_x(+\infty) > 0, \quad (34)$$

[see the first of Eqs. (28)], i.e., the background nonlinear plane wave cannot produce a nonlinear dielectric response overcoming the linear part. As opposed to the case discussed in Sec. IV A, in the present situation there are two distinct families of nonlinear guided waves corresponding to the ranges $\gamma > 0$ and $\gamma < -1$ (see the second column of Table I). In Fig. 5 we report different nonlinear guided wave profiles together with their power flows for different values of $\gamma > 0$ and for $u_{x\infty} = \sqrt{0.4}$. From Fig. 5(a) we note that, in this regime, the profile of u_x has a peak and a hole (around $\xi = 0$) for small and large values of γ , respectively. This behavior is easily understood since for $\gamma = 0$ we have $\beta = 0$ [from the first of Eqs. (28)] and $u_x(0) = 1 > u_{x\infty}$ (from the first of Eqs. (23) evaluated at $\xi = 0$ and for $\sigma_\epsilon = -1$) whereas, for $\gamma \rightarrow +\infty$ we have $\beta \rightarrow \sqrt{2(1 - 2u_{x\infty}^2)}$ and $u_x(0) = 0 < u_{x\infty}$ [from the limit $\gamma \rightarrow +\infty$ of the first of Eqs. (23) for $\sigma_\epsilon = -1$]. As a consequence there must be a value of γ for which u_x is uniform. Requiring that $u_x(\xi) = u_{x\infty}$, Eqs. (23) can be cast in the form

$$\begin{aligned} \beta \frac{du_z}{d\xi} &= (1 - \gamma) (-u_{z\infty}^2 + u_z^2) u_{x\infty}, \\ \frac{d^2 u_z}{d\xi^2} &= (1 + \gamma) (-u_{z\infty}^2 + u_z^2) u_z \end{aligned} \quad (35)$$

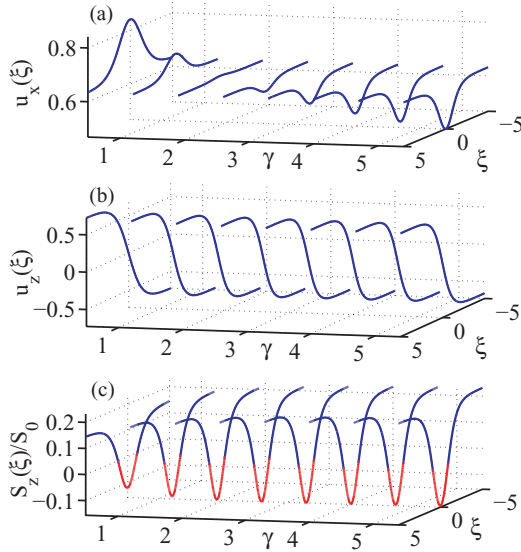


FIG. 5. (Color online) Profiles of (a) u_x , (b) u_z , and (c) S_z/S_0 of various nonlinear guided waves with $\sigma_\epsilon = -1$ and $\sigma_\mu = -1$ and $\gamma > 0$. All the waves are characterized by the same asymptotical value $u_{x\infty} = \sqrt{0.4}$.

so the solution of the second of Eqs. (35) fulfilling the boundary conditions of Eqs. (27) is

$$u_z(\xi) = u_{z\infty} \tanh \left[\sqrt{\frac{1+\gamma}{2}} u_{z\infty} \xi \right] \quad (36)$$

or, in other words, the longitudinal component u_z is an exact electromagnetic dark soliton. However, the obtained u_z has to satisfy the full Maxwell system so that, substituting the field in Eq. (36) into the first of Eqs. (35), it is straightforward to prove that this is possible only if

$$\gamma_{\pm} = \frac{1}{2u_{x\infty}^2} \left[1 \pm \sqrt{1 - 4u_{x\infty}^4} \right]. \quad (37)$$

For $u_{x\infty} = \sqrt{0.4}$ we obtain $\gamma_+ = 2$ which is the value of γ at which u_x is uniform in Fig. 5(a). Note that the situation where u_x is uniform and u_z is a dark soliton is possible only in the extreme nonlinear regime where the nonlinearity Ψ_z can compensate the linear part in the second of Eqs. (23). From Fig. 5(c) it is evident that every considered waves exhibit the transverse power flow reversing discussed in Sec. III B. The reversing of the power flow along the transverse profile of the nonlinear guided waves is particularly evident from Fig. 6 where we draw the vector field \mathbf{S} on the plane (ξ, ζ) for one of the fields of Fig. 5.

In Fig. 7 we report different nonlinear guided waves profiles together with their power flows for different values of $\gamma < 0$ and for $u_{x\infty} = \sqrt{0.4}$. Let us consider, in this case, the behavior of the nonlinear guided waves for large values of $|\gamma|$. From Figs. 6(a) and Figs. 6(b) it is evident that a kind of saturation occurs, i.e., u_x and u_z approaches their asymptotic profiles for $\gamma \rightarrow -\infty$. This is consistent with the fact that, taking the limit $\gamma \rightarrow -\infty$ of Eqs. (28) we obtain

$$\begin{aligned} \beta^2 &= 2(1 - 2u_{x\infty}^2) \\ u_{z\infty}^2 &= u_{x\infty}^2, \end{aligned} \quad (38)$$

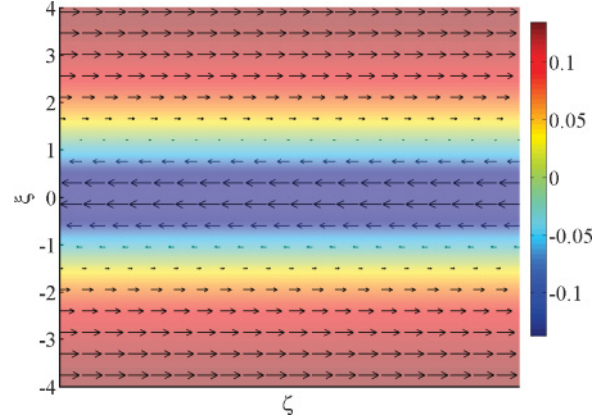


FIG. 6. (Color online) Plot of the field \mathbf{S}/S_0 (arrows) in the plane (ξ, ζ) corresponding to the nonlinear guided wave with $\gamma = 1$ of Fig. 5. The color is related to the local value of S_z/S_0 . Note the reversing of \mathbf{S} along the transverse ξ axis.

i.e., β^2 and $u_{z\infty}^2$ asymptotically approaches two finite asymptotic values and it is relevant that $u_{z\infty}^2 \rightarrow u_{x\infty}^2$. In order to obtain the asymptotic profiles of u_x and u_z , we note that, taking the limit $\gamma \rightarrow -\infty$ of Eqs. (23) and consistently assuming that the profiles remains everywhere finite, consistency requires that $u_x^2(\xi) = u_z^2(\xi)$ so that, asymptotically, $u_x(\xi) = u_z(\xi)$ for $\xi < 0$ and $u_x(\xi) = -u_z(\xi)$ for $\xi > 0$ (since u_x and u_z are spatially even and odd, respectively). Exploiting this property, Eqs. (23) yields, for $\gamma \rightarrow -\infty$, the equation

$$\frac{d^2 u_z}{d\xi^2} = 4(-u_{x\infty}^2 + u_z^2) u_z \quad (39)$$

so that, the asymptotic nonlinear guided wave profiles are

$$\begin{aligned} u_x(\xi) &= |u_{x\infty} \tanh(\sqrt{2} u_{x\infty} \xi)|, \\ u_z(\xi) &= -u_{x\infty} \tanh(\sqrt{2} u_{x\infty} \xi). \end{aligned} \quad (40)$$

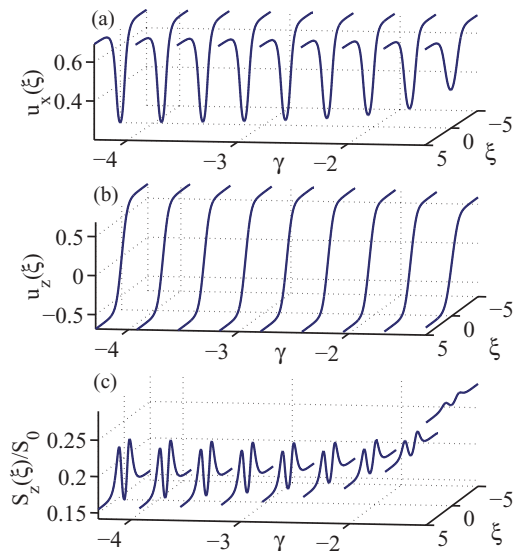


FIG. 7. (Color online) Profiles of (a) u_x , (b) u_z , and (c) S_z/S_0 of various nonlinear guided waves with $\sigma_\epsilon = -1$ and $\sigma_\mu = -1$ and $\gamma < -1$. All the waves are characterized by the same asymptotical value $u_{x\infty} = \sqrt{0.4}$.

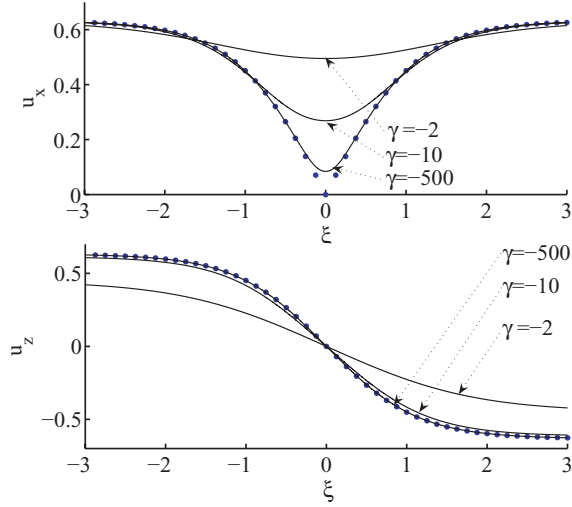


FIG. 8. (Color online) Profiles of u_x and u_z (solid lines) of nonlinear guided waves for $u_{x\infty} = \sqrt{0.4}$ and $\gamma = -2, -10, -500$. The asymptotical ($\gamma \rightarrow -\infty$) profiles of Eqs. (40) are also reported (dotted line).

Note that the asymptotic profile of u_x is singular at $\xi = 0$ (i.e., it is continuous but not differentiable) as a consequence of the unrealistic assumption $\gamma \rightarrow -\infty$. Even though the profiles of Eqs. (40) are not physical, they show that both u_x^2 and u_z^2 asymptotically approach the square of an electromagnetic dark soliton and they provide a very good description of the above-mentioned saturation for $\gamma < 0$. The profiles of u_x and u_z for $u_{x\infty} = \sqrt{0.4}$ and $\gamma = -2, -10, -500$ together with the asymptotical profiles of Eqs. (40) are plotted in Fig. 8, from which it is evident that, for $\gamma < -10$, the asymptotical profiles of Eqs. (40) accurately describe the actual field profiles (apart from a small region around $\xi = 0$ for u_x). We conclude that, in the extreme nonlinear regime, the compensation between Ψ_x and Ψ_z and the linear terms, if $|\gamma| \gg 1$, forces u_x^2 and u_z^2 almost to coincide.

$$\begin{aligned} \beta \frac{du_z}{d\xi} &= (\beta^2 - \sigma_\epsilon \sigma_\mu) u_x - \sigma_\mu [(1 + \gamma) u_x^2 + (1 - \gamma) u_z^2] u_x, \\ \beta \frac{du_x}{d\xi} &= \frac{\beta^2 \sigma_\epsilon + (1 - \gamma) \{ (2\sigma_\epsilon \sigma_\mu - \beta^2) + 2\sigma_\mu [(1 + \gamma) u_x^2 + (1 - \gamma) u_z^2] \} u_x^2 + \beta^2 (1 + \gamma) u_z^2}{\sigma_\epsilon + [3(1 + \gamma) u_x^2 + (1 - \gamma) u_z^2]} u_z, \end{aligned} \quad (\text{A1})$$

which is a system of ordinary differential equations equivalent to Maxwell equations provided the relation

$$\sigma_\epsilon + [3(1 + \gamma) u_x^2 + (1 - \gamma) u_z^2] \neq 0 \quad (\text{A2})$$

holds along the whole profile $u_x(\xi), u_z(\xi)$ [38]. The system of Eqs. (A1) can be fully analytically investigated since it admits the first integral

$$\begin{aligned} F(u_x, u_z) &= [(\beta^2 - \sigma_\epsilon \sigma_\mu) u_x^2 - \sigma_\epsilon \sigma_\mu u_z^2] \\ &\quad - \frac{1}{2} \sigma_\mu (1 + \gamma) (u_x^4 + u_z^4) - \sigma_\mu (1 - \gamma) u_x^2 u_z^2 \end{aligned}$$

V. CONCLUSIONS

In conclusion, we have investigated the effective response of a nonlinear Kerr metamaterial obtained by homogenizing a one-dimensional layered periodic structure. The effective response formally coincides with that of a standard nonlinear Kerr medium with the important difference that its parameters (both linear and nonlinear) can be independently designed and that they can assume even values not achievable in standard material. As a consequence we can choose the linear dielectric permittivity to be much smaller than 1, thus allowing the observation of the regime where the nonlinear polarization can not be regarded as a small perturbation (extreme nonlinear regime). As a leading general phenomenon characterizing the extreme nonlinear regime we have discussed the transverse power flow reversing effect, i.e., the fact that the power flow can change its sign along the transverse beam profile. Combining the extreme nonlinear regime and the fact the effective Kerr response can be tailored in an unconventional way, we have discussed a number of phenomena exploiting a class of fields (nonlinear guided waves) admitting full analytical description. Examples of such effects are the fact that the nonlinear waves can propagate even if the medium linear properties (dielectric permittivity and magnetic permeability) would forbid propagation, hyperfocusing induced by the phase difference between the field components (in the case $\gamma = -1$), and extreme compensation between the field components if they are $\pi/2$ out of phase in the limiting situation $\gamma \gg 1$.

APPENDIX: NONLINEAR GUIDED WAVES EXISTENCE

In order to derive the existence conditions of nonlinear waves satisfying Eqs. (23) and Eqs. (27), it is convenient to cast Eqs. (23) into the standard form of a first-order system of differential equations. Differentiating the first of Eqs. (23) and substituting the obtained expression of $d^2 u_z / d\xi^2$ into the second of Eqs. (23), we obtain, after some algebra,

$$\begin{aligned} & - \frac{1}{\beta^2} \{ (\beta^2 - \sigma_\epsilon \sigma_\mu) - \sigma_\mu [(1 + \gamma) u_x^2 \\ & + (1 - \gamma) u_z^2] \}^2 u_x^2 \end{aligned} \quad (\text{A3})$$

or, in other words, the relation

$$\frac{d}{d\xi} F(u_x(\xi), u_z(\xi)) = 0 \quad (\text{A4})$$

holds for any solution $u_x(\xi), u_z(\xi)$ of Eqs. (A1). Considering the boundary conditions of Eqs. (27), since $u_x(\xi)$ and $u_z(\xi)$ have to asymptotically approach two constant values, their first and second derivatives vanish for $\xi \rightarrow +\infty$ so that we require

the right-hand sides of Eqs. (A1) to vanish at $u_x = u_{x\infty}$ and $u_z = u_{z\infty}$. As a consequence we obtain

$$\begin{aligned}\beta^2 &= \frac{2\gamma\sigma_\mu}{1+\gamma}(\sigma_\epsilon + 2u_{x\infty}^2), \\ u_{z\infty}^2 &= \frac{-\sigma_\epsilon - (1-\gamma)u_{x\infty}^2}{1+\gamma},\end{aligned}\quad (\text{A5})$$

which are the relations expressing the propagation constant β and the asymptotical amplitude $u_{z\infty}$ as functions of the asymptotical amplitude $u_{x\infty}$. In addition, exploiting the fact that the $F(u_x, u_z)$ is constant along the wave profile, the relation

$$F(u_{x0}, 0) = F(u_{x\infty}, u_{z\infty}), \quad (\text{A6})$$

in which β and $u_{z\infty}$ have been eliminated using Eqs. (A5), is a cubic equation for u_{x0}^2 which can be solved to yield the peak amplitude u_{x0} as a function of the asymptotical amplitude $u_{x\infty}$.

For each $u_{x\infty}$, the existence of the corresponding guided waves has to be assured by a number of requirements. In first place β and $u_{z\infty}$ have to be real so, from Eqs. (A5),

we obtain

$$\begin{aligned}\frac{\gamma\sigma_\mu(\sigma_\epsilon + 2u_{x\infty}^2)}{1+\gamma} &\geq 0, \\ \frac{-\sigma_\epsilon - (1-\gamma)u_{x\infty}^2}{1+\gamma} &\geq 0,\end{aligned}\quad (\text{A7})$$

which are necessary inequalities for guided waves existence. Analogously, it is necessary that u_{x0} , obtained by Eq. (A6), is real. On the other hand, the above boundary conditions for $\xi \rightarrow +\infty$ imply that, after substituting the expression of β^2 of the first of Eqs. (A5) into Eq. (A3), the function $F(u_x, u_z)$ has a stationary point at $(u_{x\infty}, u_{z\infty})$. Therefore, since the curve $(u_x(\xi), u_z(\xi))$ of the plane (u_x, u_z) has to reach the point $(u_{x\infty}, u_{z\infty})$, it has to be required that $F(u_x, u_z)$ has a saddle point at $(u_{x\infty}, u_{z\infty})$ and this leads to the necessary inequality

$$\begin{aligned}\left[\left(\frac{\gamma^2 + 4\gamma + 1}{1+\gamma}\right)u_{x\infty}^2 + \frac{\gamma\sigma_\epsilon}{1+\gamma}\right] \\ \times [2(1-\gamma)u_{x\infty}^4 + \sigma_\epsilon(3-\gamma)u_{x\infty}^2 + 1] > 0.\end{aligned}\quad (\text{A8})$$

We conclude that the existence of the nonlinear guided waves we are considering is assured by the condition of Eq. (A2), together with the reality of u_{x0} [obtained by solving Eq. (A6)] and the inequalities of Eqs. (A7) and (A8). The fulfillment of all these requirements leads to the existence conditions reported in Table I.

-
- [1] S. Ramakrishna and T. M. Grzegorzczuk, *Physics and Applications of Negative Refractive Index Materials* (CRC Press, 2009).
- [2] W. Cai and V. Shalaev, *Optical Metamaterials: Fundamentals and Applications* (Springer, Dordrecht, 2010).
- [3] J. B. Pendry, *Phys. Rev. Lett.* **85**, 3966 (2000).
- [4] N. Fang, H. Lee, C. Sun, and X. Zhang, *Science* **308**, 534 (2005).
- [5] J. B. Pendry, D. Schurig, and D. R. Smith, *Science* **312**, 1780 (2006).
- [6] D. Schurig, J. J. Mock, B. J. Justice, S. A. Cummer, J. B. Pendry, A. F. Starr, and D. R. Smith, *Science* **314**, 977 (2006).
- [7] N. Engheta, *Science* **317**, 1698 (2007).
- [8] A. Alu, M. G. Silveirinha, A. Salandrino, and N. Engheta, *Phys. Rev. B* **75**, 155410 (2007).
- [9] M. Silveirinha and N. Engheta, *Phys. Rev. Lett.* **97**, 157403 (2006).
- [10] R. Liu, Q. Cheng, T. Hand, J. J. Mock, T. J. Cui, S. A. Cummer, and D. R. Smith, *Phys. Rev. Lett.* **100**, 023903 (2008).
- [11] B. Edwards, A. Alu, M. E. Young, M. Silveirinha, and N. Engheta, *Phys. Rev. Lett.* **100**, 033903 (2008).
- [12] A. A. Zharov, I. V. Shadrivov, and Y. S. Kivshar, *Phys. Rev. Lett.* **91**, 037401 (2003).
- [13] I. V. Shadrivov and Y. S. Kivshar, *J. Opt. A: Pure Appl. Opt.* **7**, S68 (2005).
- [14] N. Lazarides and G. P. Tsironis, *Phys. Rev. E* **71**, 036614 (2005).
- [15] N. A. Zharova, I. V. Shadrivov, A. A. Zharov, and Y. S. Kivshar, *Opt. Express* **13**, 1291 (2005).
- [16] R. S. Hegde and H. t. G. Winful, *Opt. Lett.* **30**, 1852 (2005).
- [17] J. B. Pendry, A. J. Holden, D. J. Robbins, and W. J. Stewart, *IEEE Trans. Microwave Theory Tech.* **47**, 2075 (1999).
- [18] I. V. Shadrivov, S. K. Morrison, and Y. S. Kivshar, *Opt. Express* **14**, 9344 (2006).
- [19] S. O'Brien, D. McPeake, S. A. Ramakrishna, and J. B. Pendry, *Phys. Rev. B* **69**, 241101(R) (2004).
- [20] D. Stroud and Van E. Wood, *J. Opt. Soc. Am. B* **6**, 778 (1989).
- [21] A. E. Neeves and M. H. Birnboim, *J. Opt. Soc. Am. B* **6**, 787 (1989).
- [22] J. E. Sipe and R. W. Boyd, *Phys. Rev. A* **46**, 1614 (1992).
- [23] G. L. Fischer, R. W. Boyd, R. J. Gehr, S. A. Jenekhe, J. A. Osaheni, J. E. Sipe, and L. A. Weller-Brophy, *Phys. Rev. Lett.* **74**, 1871 (1995).
- [24] J. P. Huang and K. W. Yu, *Phys. Rep.* **431**, 87 (2006).
- [25] R. W. Boyd, *Nonlinear Optics* (Academic Press, New York, 1994).
- [26] A. Ciattoni, C. Rizza, and E. Palange, e-print arXiv:0911.1047v2.
- [27] G. Allaire, *SIAM J. Math. Anal.* **23**, 1482 (1992).
- [28] D. Felbacq, G. Bouchitté, B. Guizal, and A. Moreau, *J. Nanophoton.* **2**, 023501 (2008).
- [29] A. I. Cabuz, D. Felbacq, and D. Cassagne, *Phys. Rev. Lett.* **98**, 037403 (2007).
- [30] P. A. Belov and Y. Hao, *Phys. Rev. B* **73**, 113110 (2006).
- [31] Y. B. Feinberg and N. A. Khizhniak, *Sov. Phys. Tech. Phys.* **27**, 2006 (1957).

- [32] S. A. Ramakrishna and J. B. Pendry, *Phys. Rev. B* **67**, 201101(R) (2003).
- [33] W. Boyd and J. E. Sipe, *J. Opt. Soc. Am. B* **11**, 297 (1994).
- [34] R. E. Noskov and A. A. Zharov, *Opto-electronics review* **14**, 217 (2006).
- [35] A. Husakou and J. Herrmann, *Phys. Rev. Lett.* **99**, 127402 (2007).
- [36] M. Scalora, M. S. Syrchin, N. Akozbek, E. Y. Poliakov, G. D'Aguanno, N. Mattiucci, M. J. Bloemer, and A. M. Zheltikov, *Phys. Rev. Lett.* **95**, 013902 (2005).
- [37] Y. Hu, S. Wen, H. Zhuo, K. You, and D. Fan, *Opt. Express* **16**, 4774 (2008).
- [38] A. Ciattoni, B. Crosignani, P. Di Porto, and A. Yariv, *J. Opt. Soc. Am. B* **22**, 1384 (2005).